

¹ Dattatreya
Gopi

² Kondalu
Banavathu

³ Krishna
Dharavathu

⁴ G. V. Sridhar

⁵ Madduri
Venkatewarlu

Textile Based Wearable Neck Collar Antenna for Early Detection of Thyroid Cancer



Abstract: - A Textile-based co-planar Tri-slotted Rectangular Patch (TSRP) antenna of dimensions $100 \times 30 \times 1.05$ mm³ is proposed for early detection of the thyroid cancer. In the designing process, textile material denim is used as a substrate with dielectric constant (ϵ_r) 1.7 and the technique of DGS (Defected Ground Structure) is used to overcome the drawback of narrow bandwidth. The proposed TSRP antenna is designed for ISM (Industrial, Scientific and Medical) band applications, which covers the frequency range from (2.25 - 3) GHz and resonates at 2.41 GHz. The bandwidth and reflection coefficient of the antenna when simulated in free space are 0.75 GHz, with an S11 of -47.68 dB respectively. The gain of the TSRP antenna in free space is 2.62dBi. The characteristics of the antenna are varied when placed on the thyroid gland. When the TSRP antenna is placed on the human tissue without tumor, it resonates at 2.12 GHz frequency and covers the range of (1.61 - 2.72) GHz frequency whereas with tumor, it resonates at 2.17GHz frequency and covers the range of (1.66 to 2.71) GHz frequency. The gain and reflection coefficient of antenna when simulated on body without tumor are -8.81 dBi, -16.61dB. Similarly, with tumor the gain and reflection coefficient are 3.63dBi, -14.62dB. The antenna is said to be helpful for thyroid cancer detection because, the reflection coefficient shows variation when placed on with and without tumor cells. The main lobe magnitude of the antenna is observed as 2.31dBi for E-plane and -2.44dBi in H-plane. SAR (Specific Absorption Rate) for the antenna in bent state when simulated on Body without tumor is 1.77 W/kg. The TSRP antenna is simulated using CST (Computer Software Technology) Simulation software.

Keywords: CPW (Co-planar waveguide), DGS (Defected ground structure), ISM (Industrial, Scientific and Medical), SAR (Specific Absorption Rate), Wearable Antenna.

I. INTRODUCTION

Wearable Antennas are becoming popular nowadays. The technological development in the antennas spreads to new industries like Biomedical, Aeronautical, Space, Military [1], [2], [3], [4], [5], [6] etc. Due to the advancement in antenna technology, we are more attracted towards textile-based antennas which can be used for bio-medical applications. The concept of wearable textile antennas is focused at improving human life quality by providing them with several wearable continuous monitoring applications [7], [8]. These wearable antennas using textile as a substrate can be easily integrated into clothes. The low dielectric constant of these textile-based substrates helps us reduce the surface wave losses and also improve the bandwidth of the antenna [9]. Even though we have many conventional antennas like Yagi Uda, Horn etc., these are not suitable for conformal applications because of this many microstrip patch antennas are introduced and considered as best suitable for wearable applications [10], [11].

The main drawback of microstrip patch antenna is Narrow bandwidth and we can overcome this with the help of many techniques like DGS, EBG, CPW[12] etc. The CPW technique is employed for the enhancement of bandwidth [13], Better impedance matching, Better reflection coefficient and reduction of back lobe losses [14], [15]. The antennas are made compact to make them easily self-Adaptable. Apart from microstrip antennas, wireless body area networks (WBAN), Printed circuit boards (PCB) are also one of the most researched interests [16]. The main drawback of the PCB is flexibility. The antenna is directly affected by the thickness of the substrate, dielectric constant, so attention must be paid to them while designing the antenna. The first and foremost challenge faced while designing is operating them at Low frequency ranges without affecting their gain and radiation efficiency. To increase the current path is the effective solution in order to overcome the difficulties such as reduction in bandwidth, degradation of gain. In Another aspect, the researchers are recently attracted towards the materials like polyimide substrates because of the fact that they have excellent mechanical properties including their light weight, durability, tensile strength, flexibility, high heat resistance, high moisture release,

^{1,4} Dept., of ECE, Raghu Engineering College, Vizag, A.P, India

² Dept., of ECE, NRI Institute of Technology, Krishna Dt., A.P, India

^{3,5} Dept., of ECE, PSCMR College of Engineering and Technology, Vijayawada, Andhra Pradesh, India

* Corresponding Author Email: ¹dattatreya.gopi@gmail.com, ²kondalu.phd@gmail.com, ³krishnadharavath4u@gmail.com,

⁴sridhar1209@gmail.com, ⁵pragna2004@gmail.com

Copyright © JES 2024 on-line: journal.esrgroups.org

low moisture uptake, excellent electrical properties. So, they want to include them in their designs for wearable antennas.

With the increase in demand for the wearable biomedical antennas, the researchers have shown great interest in them because of that these antennas are working better than several medical devices, when embedded in textile materials [17], [18, 19]. In order to build these high quality biomedical devices the researchers have designed several antennas to match the required performance. However, even after designing antenna with wearable materials, the wearable antenna should undergo different analysis and test such as Antenna size, low weight, Power consumption, Gain, SAR for the compatibility on human body[20].

In addition, even though many modifications have been done the obstacles of constructing and operating a textile antenna on the human body are numerous, such as the effect of their location on human body, the amount of radiation emitted, reliability losses due to Antenna deformation and Electromagnetic leakages from wearable antenna towards the human body. Steps must be taken to guarantee that the performance does not deteriorate significantly.

II. ANTENNA DESIGN ANALYSIS

The proposed TSRP antenna design is used for biomedical applications. And while designing it there are certain steps to be followed. Firstly, select a frequency range from ISM bands as an operating frequency for the proposed antenna. Secondly, select a substrate material suitable for the wearable applications. These are needed to determine the dimensions. For the proposed antenna the frequency band of 2.4 to 2.45 GHz and denim having permittivity (ϵ_r) of 1.7 and tangent losses (δ) of 0.020 are considered as a substrate. The dimensions of the radiating patch are determined by λ_g .

Where λ_g Is guide wavelength [21] i.e.,

$$\lambda_g = \frac{c}{f \times \sqrt{e_{eff}}} \tag{1}$$

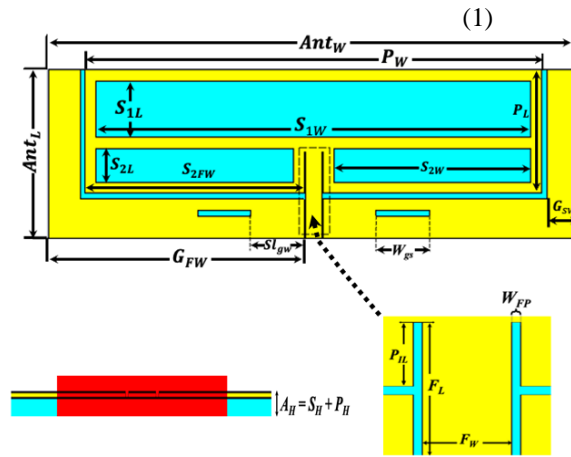


Fig. 1. Geometry of TSRP antenna.

Fig. 1 shows the geometry of the proposed antenna. The dimensions of proposed antenna are reduced to 30×30 mm² in order to make the antenna suitable for our requirement. And DGS has been used for enhancing the bandwidth, slots are considered at point where the feed line meets the radiating patch of antenna in order to match the impedance. In order to get the desired band of frequency evolution process is considered for the proposed TSRP antenna as shown in Fig.2.

Table I: Dimensions of proposed TSRP antenna

Geometrical Parameters	Values (Mm)	Geometrical Parameters	Values (Mm)
Antw	100	S1L	10
AntL	30	S1W	82
Pw	86	S2L	6
PL	22	S2W	37.20
GFW	48.20	S2FW	41.20
GSW	6	W _{gs}	0.30
A _H	1.05	S _H	1.0
P _H	0.05	P _{IL}	7.30
F _L	15.03	F _W	3.00

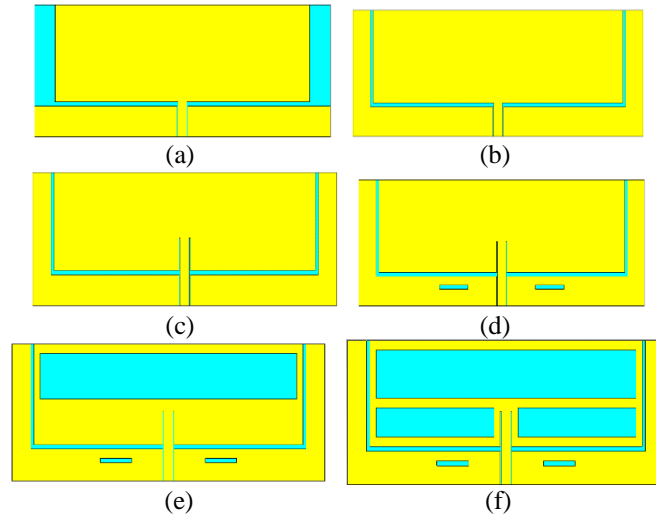


Fig. 2. Proposed TSRP antenna evolution process

2.1 *TSRP Antenna in Free Space*

The Fig. 3(a) represents proposed TSRP antenna in planer state and is observed in free space to ensure the antenna is radiating in ISM Band. Similarly the performance of the antenna is also observed when it is subjected to bending with an angle of 32° as shown in Fig. 3(b) to make sure its operating frequency lies between ISM Band and are also similar when compared with TSRP antenna in planer state.

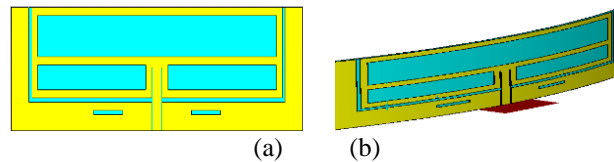


Fig. 3. Proposed TSRP antenna in (a) Planar state, (b) Bent state

2.2 *TSRP Antenna with Human Tissues*

The proposed TSRP antenna is a wearable antenna which can be incorporated into the collar or can be used in neckband, so it becomes mandatory to observe the performance of the antenna when placed on human tissue. In order to perform the analysis, simulated human thyroid tissue model is designed as shown in Fig. 5 with a dimension of 140×50mm² which includes skin, fat, muscle, thyroid gland and tumor on which the antenna is placed. Fig. 4(a) represents antenna in planer state when placed on thyroid tissue model whereas Fig. 4(b) represents the bent state of antenna placed on tissue model.

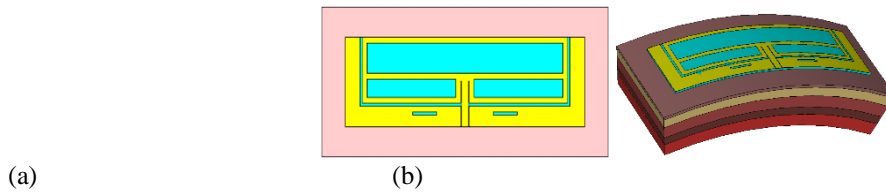


Fig. 4. Proposed TSRP antenna with simulation human tissue.



Fig. 5. Human Thyroid Tissue model for the proposed TSRP.

Each layer of the tissue model have a different Permittivity (ϵ_r), Tangent loss, Conductivity and Density as shown in table 2 i.e. for skin the ϵ_r is 31.29 and Tangent losses is 0.2835, fat ϵ_r is 5.28 and Tangent losses 0.19382, muscle ϵ_r is 52.79 and Tangent losses of 0.24191, thyroid ϵ_r is 1.5 and conductivity is 1.469 [22]. The thickness of this layers also varies, the top most layer being skin has a thickness of 1.5 mm followed by fat of thickness 4.5 mm and next layers Muscle, thyroid and tumour has a thickness of 6mm ,4mm, 6mm as shown in table 2(a) and 2(b).

Table II(a): Human tissue simulation model properties

Tissue Layers	ser	Conductivity (S/M)	Tangent Losses (Tan σ)
SKIN	31.29	5.0138	0.2835
FAT	5.28	0.1	0.19382
MUSCLE	52.79	1.705	0.24191
THYROID	1.5	1.469	-
TUMOR	4.5	6	-

Table II(b): Human tissue simulation model Parametric values

PARAMETER	HS	HF	HM	HT	HTU
VALUES (mm)	1.5	4.5	6	4	6

III. RESULT AND ANALYSIS

In order to get the desired band of frequencies, evolution process is considered as shown in Fig. 2. Fig. 6 shows the change in operating frequency, reflection coefficient, and bandwidth. Fig. 2(a), Ant.1 is initial stage represents a basic patch antenna which is rectangle in shape with dimensions of (86mm×22mm) and is resonating at 2.65 GHz with a Reflection coefficient of -12.748dB. In Fig. 2(b) the Ant. 2 ground is extended on the left and right side of the antenna patch as resulted in frequency shift at 2.66 GHz.

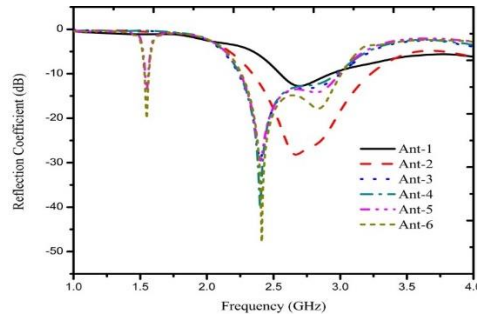


Fig. 6. S11 response of the evolution process.

In Fig. 2(c) i.e. Ant-3 slots are added in between feed and patch to match the impedance. This results in shift of frequency of the antenna to 2.401 GHz with a reflection coefficient of -29.24dB. Fourth Stage Ant.4 involves adding of slots to the ground as shown in Fig. 2(d) which resulted in enhancing the bandwidth and reflection coefficient of the proposed antenna. Three different slots are added to the antenna patch in Ant.5 and Ant.6 as shown in Fig. 2(e) & Fig. 2(f) in order to obtain an S11 of -47.6dB at 2.413GHz frequency.

Table III: Antenna evolution process parameters

TSRP antenna evolution	Resonating Frequency (GHz)	Frequency Range (GHz)	Reflection coefficient S11 (dB)
Ant-1	2.60	2.5-2.9	-12.7
Ant-2	2.66	2.34-3.23	-28.17
Ant-3	2.401	2.23-3.00	-29.24
Ant-4	2.401	2.24-2.97	-40.22
Ant-5	2.401 & 1.549	(2.25-2.99) & (1.53-1.56)	-29.53 & -13.55
Ant-6	2.413 & 1.549	(2.25-3.00) & (1.53-1.56)	-47.68 & -20.05

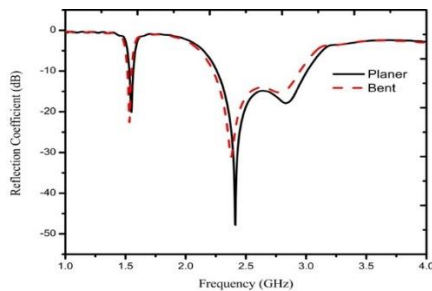


Fig.7. Reflection coefficient of proposed antenna in planer and bent state in free space.

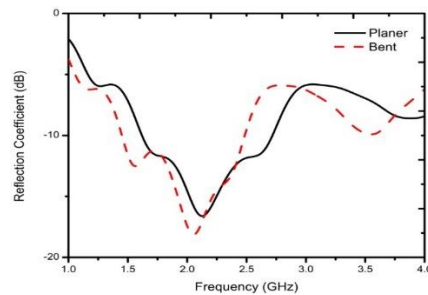


Fig. 8. Reflection coefficient of proposed antenna in planer and bent state without tumour.

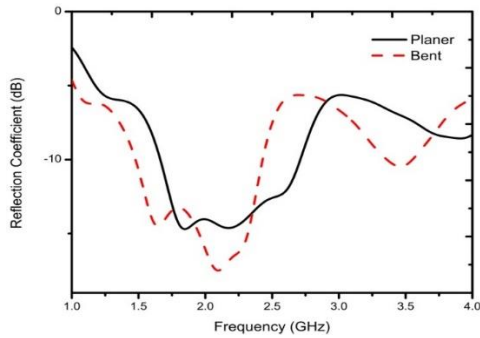


Fig.9. Reflection coefficient of proposed antenna in planer and bent state with tumour.

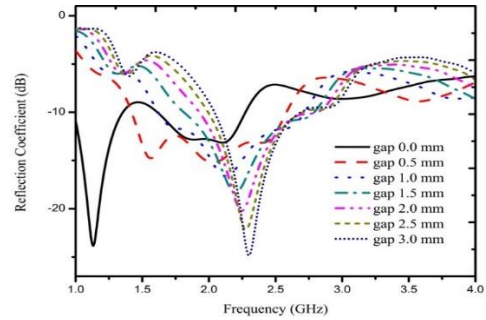


Fig. 10. Reflection coefficient of proposed antenna in planer state without tumour and different air gaps.

Fig. 7 shows the reflection coefficient of proposed antenna in both the planer and bent state in free space. The solid line indicates the reflection coefficient S_{11} of proposed antenna in planer state and dashed line indicates the reflections coefficient of antenna in bent state. Proposed antenna in planer state is resonate at two frequency i.e. 1.5 GHz and 2.4 GHz with a frequency range of (1.53 GHz to 1.56 GHz), (2.25 GHz to 3 GHz) with a bandwidth of 30MHz and 750MHz whereas antenna in bent state is resonating at two different frequencies i.e. 1.51 GHz and 2.29 GHz with a frequency range of (1.50 GHz to 1.53 GHz) and (2.16 GHz to 2.83 GHz) and the bandwidth is 0.3 GHz and 0.67 GHz as mentioned in FIG. 8 shows the reflection coefficient S_{11} of proposed antenna in both the planer and bent state without tumor. The solid line indicates antenna in planer state and dashed line indicates antenna in bent state when placed on human tissue without tumor. Antenna in planer state and bent state are resonating at frequencies 2.12 GHz and 2.05 GHz and the S_{11} is observed as -16.6dB and -18.1dB with a frequency range of (1.61 to 2.72 GHz) and (1.44 to 2.48 GHz) and with a bandwidth of 1.11 GHz and 1.04 GHz respectively, and it is observed in Fig.9 that some deviations are observed when placing antenna on thyroid tumor and the observed results are 2.17 and 2.12 GHz , -14.62 and 17 dB , (1.66 – 2.17 GHz) and (1.47 – 2.48 GHz) , 0.51and 1.01 GHz. Table 4 indicates the Parameters of Planer and Bent antenna in different operating states.

Fig. 10 represents the reflection coefficient of proposed antenna in the planer state with different air gaps as mentioned in Table 4. Without air gap a bandwidth ranging from (0.9 to 1.3) GHz is observed with an S_{11} of -24dB when the air gap is increased to 0.5mm the Bandwidth ranging is increased to (1.5 - 2.5) GHz with S_{11} of -15.19dB. Similarly when the air gap is increased to 1mm, 1.5mm, 2mm, 2.5mm, 3mm it is observed that the bandwidth and SAR are decreasing whereas the s_{11} is increasing.

Table IV: Parametric Analysis of proposed antenna.

Gap (mm)	Frequency (GHz)	Bandwidth (GHz)	Reflection coefficient(dB)	Gain	SAR
0	1.61 – 2.27	0.66	-13.14	-11.1	4.85
0.5	1.42 – 2.58	1.16	-15.19	-9.87	3.74
1.0	1.61 – 2.71	1.10	-16.61	-8.81	3.67
1.5	1.81 – 2.79	0.98	-18.33	-7.6	3.17
2.0	1.92 – 2.81	0.89	-20.13	-6.67	2.17
2.5	1.99 – 2.70	0.71	-22.18	-5.96	2.31
3	2.04 – 2.68	0.64	-24.79	-5.38	2.01

Table V: Parameters of Planer and Bent antenna in different operating states.

Operating State	Frequency (GHz)	Bandwidth (Ghz)	S11(dB)	Gain(dB)	SAR(W/kg)
Planar Free Space	2.41 (2.25– 3.00) & 1.54(1.53 – 1.56)	0.75 & 0.03	-40.40	2.62	–
Planar on Body with out tumour	2.12(1.61 – 2.72)	1.11	-16.61	-8.81	3.67
Planar on Body with tumour	2.17(1.66 – 2.71)	1.05	-14.62	3.63	3.63
Free Space with bending	2.29(2.16 – 2.83) & 1.51(1.50 – 1.53)	0.67 & 0.03	-33.77 & -18.05	2.17	–
Tissue withoutTumour (with bending)	2.05(1.44 – 2.48)	1.04	-18.13	-8.78	2.27
Tissue with tumour (with bending)	2.09(1.47 – 2.42)	0.95	-17.20	-8.93	1.77

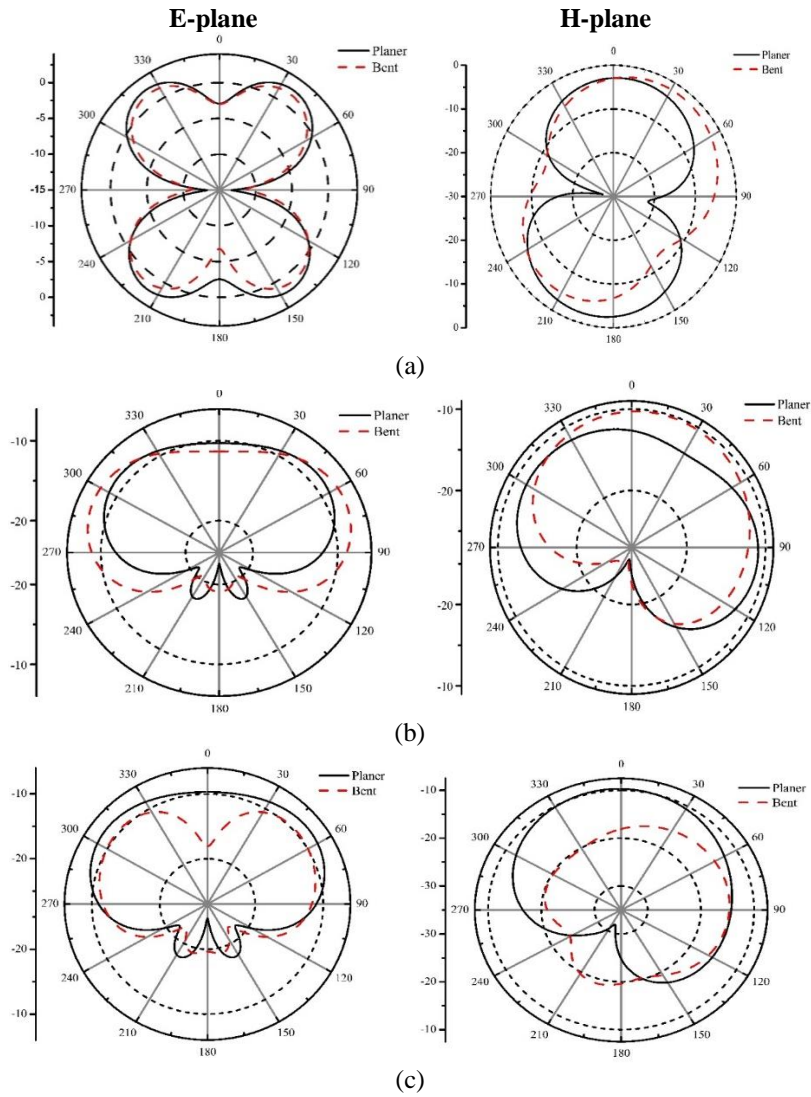


Fig. 11. Radiation pattern of Planar and Bent Antenna in all operating states

Fig. 11(a-c) represents the E and H field radiation patterns of the proposed antenna for planar, bent and tissue models. Planer antenna is indicated with solid line and bent antenna is indicated with dotted line. Fig. 11(a) represents the E-field and H-field of planer and bent antenna in free-space. For E-field planer antenna is radiating with Main lobe magnitude of 2.31dBi in the direction of 36.0deg whereas the bent antenna is radiating at an angel of 35.0deg with a Main lobe Magnitude of 1.58dBi, and Angular width (3dB) of both antennas are 48.7deg and 49.4 deg. Similarly for the H-field the planer antenna has Main lobe Magnitude of -2.44dBi at 193.0 deg, whereas the bent antenna has a main lobe Magnitude of -1.78 which is radiating at 34.0deg. Fig. 11(b), Fig 11(c) indicate E and H field for antenna in planer and bent state when placed on tissue without tumor and with tumor respectively. The analysis is show in Table-6.

Table VI: Radiation Pattern analyses of planer and bent antenna in different operating State.

	Operating State	Operating Frequency (GHz)	Mainlobe magnitude (dBi)	Main lobe direction (deg)	Angular width(3dB) (deg)
Planer E-plane	Free Space	2.45 GHz	2.31	36.0	48.7
	On tissue without tumour	2.45 GHz	-8.92	278.0	104.8
	On tissue with tumour	2.45 GHz	-9.53	52.0	201.6
Planer H-plane	Free Space	2.45 GHz	-2.44	193.0	90.0
	On tissue without tumour	2.45 GHz	-10.9	94.0	239.7

	On tissue with tumour	2.45 GHz	-9.96	70	161.9
Bent E-plane	Free Space	2.45 GHz	1.58	35.0	49.4
	On tissue without tumour	2.45 GHz	-8.83	274.0	101.1
	On tissue with tumour	2.45 GHz	-9.74	312.0	81.5
Bent H-plane	Free Space	2.45 GHz	-1.78	34.0	104.1
	On tissue without tumour	2.45 GHz	-12.5	95.0	98.5
	On tissue with tumour	2.45 GHz	-14.5	76.0	128

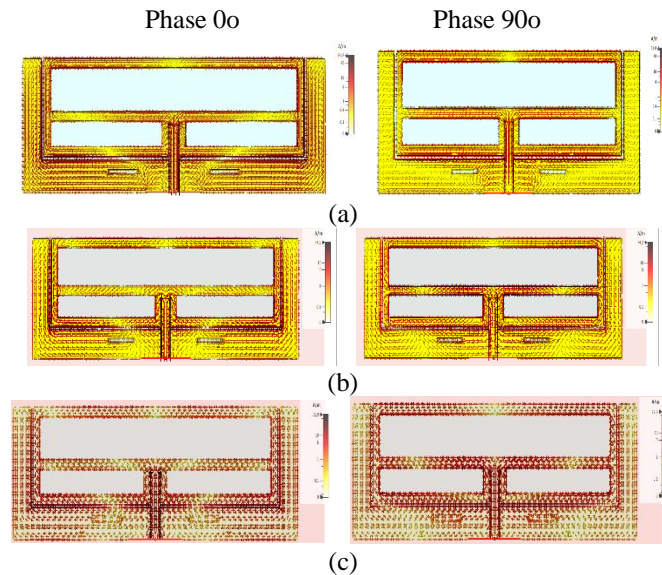
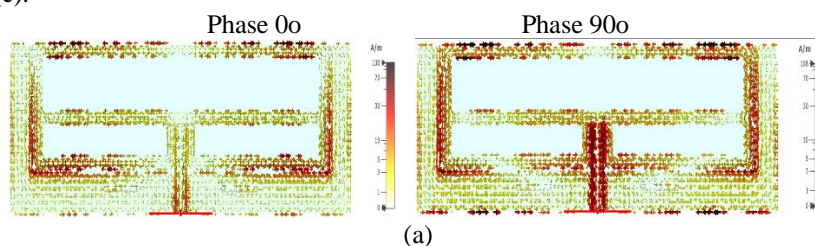


Fig. 12. Surface current distribution of TSRP antenna model in Planer mode (a) free space, (b) On tissue model without tumor, (c) On tissue model with tumor.

Fig. 12 indicates the surface current distribution of all TSRP antenna models in planer state at two different phase angles i.e., phase 0° and 90° . the surface current for these models are observed as 81.8 A/m for free space antenna at a phase angle of 0° and the maximum current is observed near the feed line, inner edges of the ground whereas at phase 90° the maximum current is observed at the edges of the patch as shown in fig. 12 (a), when the TSRP is placed on the tissue model without tumor as shown in Fig.12 (b) the surface current is observed as 74.2 A/m, at phase 0° the surface current is maximum at the bottom edge at the patch whereas at 90° maximum current is observed inner edges of the three slots of the patch. Similarly, when the antenna is placed on tissue model with tumor the maximum surface current is observed as 72.9 A/m as mentioned in Fig. 7 (c). The surface current tends to change when the proposed antenna is subjected to bending.

Fig. 13 (a-c) indicates all models of the TSRP antenna in bent state and in Fig. 13 (a) the surface current is observed as 108 A/m for antenna where the maximum current at phase 0° is observed on the side edges of the patch when compared to 90° the maximum current is observed near the feed line and on the outer edges of the patch. The surface current is re induced to 85.9 A/m when it is placed on human tissue model without tumor and it is observed that the surface current is evenly distributed over the surface but in phase 90° the surface current is density is reduced at some points on the patch and ground of the antenna as shown in Fig. 13(b). Similarly, when the TSRP antenna is placed on human tissue model with tumor it is observed that the maximum current is increased to 91.4 A/m and the surface current density is comparatively higher at phase 0° than at phase 90° as shown in Fig. 13(c).



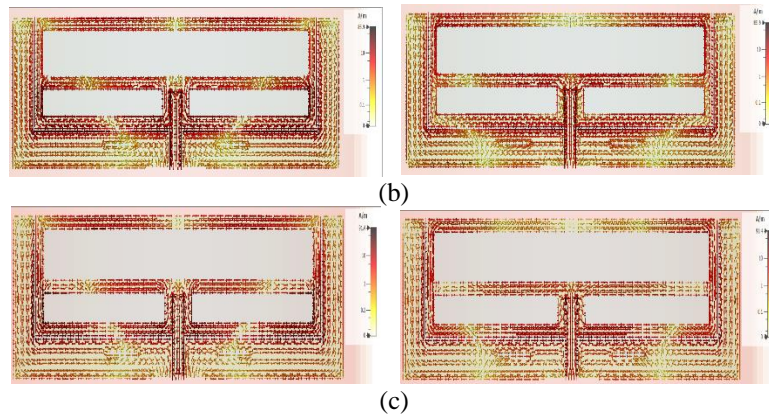


Fig. 13. Surface current distribution TSRP antenna model in bent states, (a) free space, (b) On tissue model without tumor, (c) On tissue model with tumor.

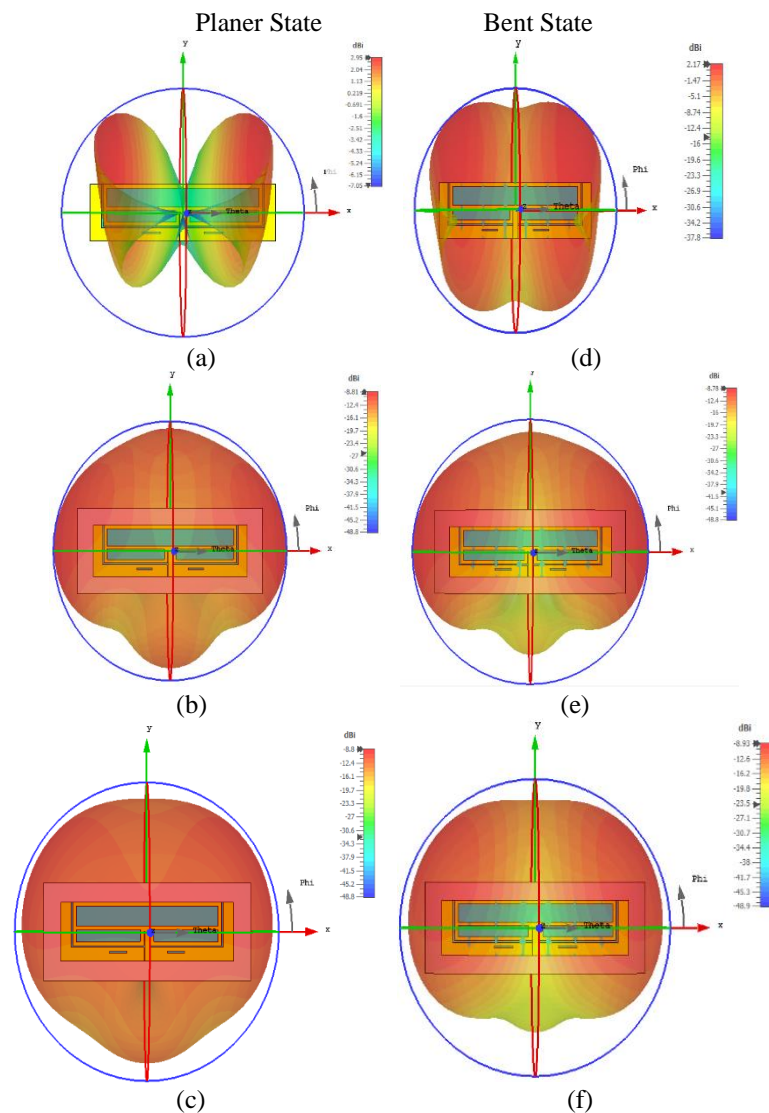


Fig. 14. Gain of TSRP antenna bent and planer state.

In the above Fig. 14(a-f) the gain of the proposed antenna in both planar and bent state are shown. Fig. 14(a) shows the gain of the proposed antenna in planar Free State and it is observed that it has gain of 2.573dBi at 2.41GHz frequency. Fig. 14(b) shows the gain of the proposed antenna without tumor and it is observed that it has gain of -7.594dBi at 2.4 GHz frequency. Fig.14(c) shows the gain of the proposed antenna with tumor and it is observed that it has gain of -7.95dBi at 2.4 GHz frequency. Fig. 14(d) shows the gain of the proposed antenna in bent state and it is observed that it has gain of 2.17dBi at 2.45 GHz frequency. Fig. 14(e) shows the gain of the

proposed antenna in Bent state without tumor and it is observed that it has gain of -8.78dBi at 2.45 GHz frequency. Fig. 14(f) shows the gain of the proposed antenna in Bent state with tumor and it is observed that it has gain of -8.93dBi at 2.45 GHz frequency.

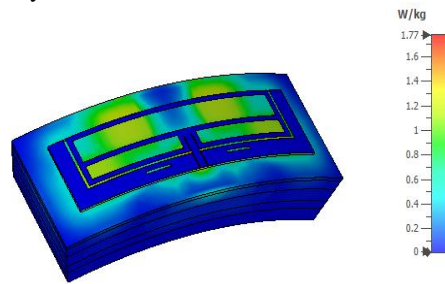


Fig. 15. SAR of proposed antenna in bent state when placed on tissue affected with tumour.

SAR (specific absorption rate) is the measurement of the amount of the RF energy which is absorbed by the human tissue. It is observed that the proposed Antenna must have a low SAR for it to be used for wearable applications. And the proposed design simulated on the human tissue to calculate the SAR value and show that it is well under the threshold Value. The SAR for the proposed antenna is 1.77w/Kg as mentioned in Fig. 15.

IV. CONCLUSION

This work demonstrates that fully functional textile antenna has strong potential to be used as biomedical antenna for early detection of thyroid cancer. The proposed TSRP antenna resonates at 2.41GHz and has the bandwidth of 0.75GHz . In free space an S_{11} of -47.68dB with a gain of 2.62dBi is observed. It is observed that the characteristics of the antenna are varied when placed on the thyroid gland of the human tissue. When the proposed TSRP antenna is placed on the human tissue without tumor, it resonates at 2.12 GHz frequency. The Gain and Reflection coefficient of antenna when simulated on Body without tumor are -8.81dBi , -16.61 dB respectively. Similarly, when the proposed TSRP antenna is placed on the human tissue with tumor, it resonates at 2.17 GHz frequency. The Gain and Reflection coefficient of antenna when simulated on Body with tumor are 3.63dBi , -14.62 dB respectively. SAR (Specific Absorption Rate) for the antenna in bent state when simulated on Body without tumor is 1.77 W/kg , which is considered safe according to IEEE standards and can be perfectly used for thyroid detection. Based on the analysis the proposed TSRP antenna is a suitable for wearable textiles for early detection of cancer tissue.

V. ACKNOWLEDGMENT

The authors would like to thank Department of ECE, KLEF, Guntur for the antenna designing and testing facilities.

REFERENCES

- [1] N. I. Zaidi et al., "Analysis on Bending Performance of the Electro-Textile Antennas With Bandwidth Enhancement for Wearable Tracking Application," *IEEE Access*, vol. 10, pp. 31800-31820, 2022.
- [2] Q. Li and H. Liu, "Research on Performance of Wearable Microstrip Antenna Based on Flexible Material," in 2021 IEEE 5th Advanced Information Technology, Electronic and Automation Control Conference (IAEAC), 2021, vol. 5, pp. 245-248: IEEE.
- [3] I. A. Chistyakov, I. S. Ozhogin, I. O. Kozhevnikov, A. M. Pavlov, A. A. Serdobintsev, and A. V. Starodubov, "Implementation of Laser Micromachining as a Promising Technique for Designing the Miniature ISM-band Flexible Coplanar Waveguide-fed Antennas," in 2021 Antennas Design and Measurement International Conference (ADMInC), 2021, pp. 10-12: IEEE.
- [4] M. H. Maktoomi, Z. Wang, H. Wang, S. Saadat, P. Heydari, and H. Aghasi, "A GSG-Excited Ultra-Wideband 103–147 GHz Stacked Patch Antenna on Flexible Printed Circuit," in 2021 IEEE International Symposium on Antennas and Propagation and USNC-URSI Radio Science Meeting (APS/URSI), 2021, pp. 1829-1830: IEEE.
- [5] S. Kiani, P. Rezaei, and M. Fakhr, "A CPW-fed wearable antenna at ISM band for biomedical and WBAN applications," *Wireless Networks*, vol. 27, no. 1, pp. 735-745, 2021.
- [6] M. Faridani, G. Xiao, R. E. Amaya, N. Javanbakht, and M. C. Yagoub, "A Kapton-Based Flexible Wideband Antenna with Metamaterial Resonators for Millimeter-Wave Wireless Applications," in 2021 IEEE International Symposium on Antennas and Propagation and USNC-URSI Radio Science Meeting (APS/URSI), 2021, pp. 1055-1056: IEEE.
- [7] S. M. Sayem and K. P. Esselle, "A Robust, Flexible and Frequency Reconfigurable Antenna with Flexible Superstrate and Substrate," in 2021 International Symposium on Antennas and Propagation (ISAP), 2021, pp. 1-2: IEEE.
- [8] D. Gopi, P. V. Kokilagadda, S. Gupta, and V. R. K. R. Dodda, "Asymmetric coplanar strip-fed textile-based wearable antenna for MBAN and ISM band applications," *International Journal of Numerical Modelling: Electronic Networks, Devices and Fields*, p. e2920, 2021.
- [9] M. N. N. Alaukally, T. A. Elwi, and D. C. Atilla, "Miniaturized flexible metamaterial antenna of circularly polarized high gain-bandwidth product for radio frequency energy harvesting," *International Journal of Communication Systems*, vol. 35, no. 3, p. e5024, 2022.

- [10] Y. Jiang, K. Pan, T. Leng, and Z. Hu, "Smart textile integrated wireless powered near field communication body temperature and sweat sensing system," *IEEE Journal of Electromagnetics, RF and Microwaves in Medicine and Biology*, vol. 4, no. 3, pp. 164-170, 2019.
- [11] J. Jenisha and K. M. Kumar, "Design Of H-Shape Microstrip Patch Antenna For Wearable Applications To Detect The Thyroid Gland Cancer Cells," *ICTACT Journal on Microelectronics*, vol. 6, no. 2, pp. 928-933, 2020.
- [12] K. Banavathu, S. Aruna, and K. S. Naik, "Conformal Lower Edge Corner Defected CPW-fed Elliptical Ring Shaped Antenna for UWB Applications," *International Journal of Microwave & Optical Technology*, vol. 17, no. 3, 2022.
- [13] G. S. Latha, G. Raju, and P. S. Dayal, "Design and Analysis Metamaterial Inspired Wearable Antenna for 2.45 GHz ISM Band," in *2020 32nd International Conference on Microelectronics (ICM)*, 2020, pp. 1-4: IEEE.
- [14] G. Wang, C. Hou, and H. Wang, "Flexible and Wearable Electronics for Smart Clothing," 2020.
- [15] M. P. Raju, D. P. Kishore, and B. Madhav, "CPW fed T-shaped wearable antenna for ISM band, Wi-Fi, WiMAX, WLAN and fixed satellite service applications," *Journal of Electromagnetic Engineering and Science*, vol. 19, no. 2, pp. 140-146, 2019.
- [16] A. Y. Ashyap et al., "Compact and low-profile textile EBG-based antenna for wearable medical applications," *IEEE Antennas and Wireless Propagation Letters*, vol. 16, pp. 2550-2553, 2017.
- [17] K. N. Ketavath, D. Gopi, and S. S. Rani, "In-Vitro Test of Miniaturized CPW-Fed Implantable Conformal Patch Antenna at ISM Band for Biomedical Applications," *IEEE Access*, vol. 7, pp. 43547-43554, 2019.
- [18] F. R. Kareem, A. A. Ibrahim, and M. A. Abdalla, "Triple band monopole textile wearable antenna for IoMT application," *IEEE Sensors Journal*, 2023.
- [19] A. B. Dey, S. Kumar, W. Arif, and J. Anguera, "Elastomeric Textile Substrates to Design a Compact, Low-Profile AMC-Based Antenna for Medical and IoT Applications," *IEEE Internet of Things Journal*, vol. 10, no. 6, pp. 4952-4969, 2022.
- [20] Ravikumar Palla, Dattatreya Gopi, Shanmukha Rao Narsupalli, "Miniaturized Wearable Antenna with Reduced Specific Absorption Rate and Enhanced Bandwidth," *SN COMPUT. SCI.* 4, 355 (2023). <https://doi.org/10.1007/s42979-023-01679-3>.
- [21] J. R. James and P. S. Hall, *Handbook of microstrip antennas*. IET, 1989.
- [22] S. Sankaralingam and B. Gupta, "Determination of dielectric constant of fabric materials and their use as substrates for design and development of antennas for wearable applications," *IEEE transactions on instrumentation and measurement*, vol. 59, no. 12, pp. 3122-3130, 2010.